Supplementary material

Materials and Methods

Tumour specimens

Samples were collected according to the BRISQ (Biospecimen Reporting for Improved Study Quality) guidelines (Moore et al., 2011). Ages of patients from whom tissue samples were collected ranged from 34 to 79 years with a median age of 59 years. Clinical follow-up of these individuals was evaluated on time to metastasis, metastasis-free survival and overall survival. This was calculated from the date of diagnosis to event or the last day of follow-up, and ranged from 3 to138 months with a mean of 27.8 months. The minimal time of follow-up for defining a metastasis-free condition was 5 years (Supplementary Table S1). 47 patients were disease-free, 61 developed metastases during the post-surgical follow-up period. 33 patients died from the disease and 7 from other causes. Tumour samples, including both primary and metastatic lesions, and 20 paired normal tissue were obtained as both frozen tissue and paraffin-embedded material and in all specimens the percentage of tumour cells estimated after hematoxylin-eosin staining of serial tissue sections was equal or more than 90%. Paired primary and metastatic (lung derived) tissues were obtained from 46 of the patients. Enrolled patients were diagnosed to suffer primary spindle cell or polymorphic STS of the following histologic subtypes: malignant fibrous histocytoma-like pleomorphic sarcoma (MHF; n = 16); leiomyosarcoma (LMS; n = 28); poorly differentiated, pleomorphic, myxoid or round-cell liposarcoma (LS; n = 47); fibrosarcoma (FS; n = 6) and monophasic synovial sarcoma (SS; n = 11). Diagnoses were according to the WHO guidelines with complementary immunohistochemical analysis of standard markers for differential diagnosis. Conventionally MFH is a diagnosis of exclusion and hence this subgroup included various types of poorly differentiated pleomorphic sarcomas. Primary tumours were all deeply localized, had a size exceeding 5 cm in diameter and were classified according to the three-wired variant of the sixth edition of the American Joint Committee for Cancer (AJCC) STS staging. The 46 metastatic specimens were consistently derived from surgically removed lung lesions.

RNA extraction and qPCR

Total RNA was extracted from tumour cell lines (~3×10^6 cells), healthy and tumour specimens (~150mg of tissue) and peripheral blood lymphocytes (~1×10^6 cells) obtained after informed consent using TRIzol Reagent (Invitrogen) and stored at –80 ℃ in RNA secure reagent (Ambion). RT of mRNA was carried out in 100 µl final volume from 400 ng total RNA using High Capacity cDNA Archive kit (Applied Biosystems) according to manufacturer's instructions. Quantitative

PCR reaction was performed on cDNA, by ABI PRISM 7900 Sequence Detector (PE Applied Biosystems), with TaqMan technology.

Expression of target genes, NG2 (CSPG4) and α3(VI) chain (COL6A3) was quantified using TaqMan Gene Expression Assays (Applied Biosystems) according to manufacturer's protocol and using Assay-on-demand primers with codes Hs99999905_m1 for GAPDH, Hs00426981_m1 for NG2 and Hs00365098_m1 for COL6A3. PCR mixture contained 1.25 μl Target or Endogenous Reference Assay Mix 20×, 22.2 ng DNA diluted in 11.25 μl of distillate water, 12.5 μl TaqMan Universal Master Mix 2× (Applied Biosystems) in a 25 ml final reaction volume. Following activation of Uracil-N-Glycosylase (UNG) for 2 min at 50 ℃ and AmpliTaq Gold DNA polymerase for 10 min at 95 ℃, all genes were amplified by 45 cycles for 15 sec at 95 ℃ and for 1 min at 60 ℃. For calculation of gene expression we used 2-ΔΔCT comparative method. The amount of target was normalized to an endogenous reference (GAPDH) and relative to a calibrator (cDNA from healthy lymphocytes). Each gene expression was considered up-regulated when the value was >1 ± standard deviation (SD) and down-regulated when the value was <1 ± SD. Value 1 corresponds to fluorescence emission in each amplification reaction for target and reference in pool of lymphocytes. SD of each 2-ΔΔct value was less than 0.2, according to protocol required for data reliability.

Immunohistochemistry and TUNEL assay

Immunohistochemical staining of human sarcoma samples was performed on formalin-fixed, paraffin-embedded specimens with a rabbit polyclonal antiserum against NG2 (antiserum D2; Virgintino et al., 2007), a panel of anti-NG2 mouse mAbs that we have recently generated using the recombinant ectodomain of the molecule as immunogen (specificitis and characteristics of these mAbs are reported elsewhere), an anti-α3(VI) chain monoclonal antibody (Novocastra), a mAb against Ki-67 (ABCAM) and a mouse mAb that we have produced in the past against human fibromodulin (clone 636B12).

The fibromodulin antibody was used in conjunction with Masson's staining to highlight the intralesional stromal content. Antibody binding was revealed with the avidin-biotin-peroxidase complex method (BIOMEDA). Surgical specimens of melanoma were used as reference. Tumour masses derived from human $NG2^+$ sarcoma cells grown in nude mice were fixed, embedded in OCT, and sectioned. The sections (7-μm thick) were incubated overnight at 4 ℃ with a rabbit polyclonal anti-NG2 antibody (1:200), an anti-α3(VI) chain monoclonal antibody (1:200), or a rabbit polyclonal anti-desmin antibody (1:200), then washed with phosphate-buffered saline (PBS) and incubated with an FITC-conjugated goat anti-rabbit IgG (1:200) or FITC-conjugates rabbit anti mouse secondary antibody (1:100, Alexa Fluor, Life Technologies, Inc.). The sections were washed

three times with PBS, mounted under coverslips in mounting medium and examined with the use of a fluorescence microscope. TUNEL assays on tumour sections were performed using the In Situ Apoptosis Detection Kit-Fluorescein TUNEL-based Apoptosis Detection Assay (R&D System) according to manufacturer's protocol.

ECM substrates

For the isolation of native matrices, the cells were extensively rinsed with Dulbecco's PBS at room temperature and then treated on ice for three periods of 10 min according to a modified procedure (Hedman et al., 1979); Nicolosi et al., in preparation), using 0.2% sodium deoxycholate (DOC) in 10 mM Tris-Cl buffered saline, pH 8.0, supplemented with a cocktail of proteinases inhibitors including 1 mM 4-(2-Aminoethyl) Benzene Sulfonyl Fluoride hydrochloride (AEBSF), 5 mg/ml 6-aminohexanoic acid, 100 nM antipain, 800 nM aprotinin, 100 μM chymostatin, 10 μM E-64, 1μM N-ethylamide, 100 μM leupeptin, and 1 μg/ml pepstatin (Sigma-Aldrich). Cell dishes were then gently washed 3 times for 10 minutes each on ice with a low ionic strength buffer (2 mM Tris-HCl, pH 8.0) containing the above proteinases inhibitors. Extreme care was taken during pipeting of the solution to avoid detachment of their matrix and to preserve the coverslips on ice. Isolated matrices were visualized by phase-contrast microscopy with anti-murine Col I (Millipore) and anti-murine Col VI (ABCAM) antibodies. For immunolabelling, samples were fixed in cold methanol (–20 ℃) for 7 min, washed in PBS and incubated for 15 min at 4 ℃ with blocking solution (PBS with 0.1% BSA). Samples were then incubated overnight at 4 ℃ with anti-murine fibronectin (BD), anti-murine Col VI (produced in the laboratory), or anti-human Col I polyclonal antiserum (Millipore Corp.) followed by FITC-conjugated antibody reaction (1 h at 4 ℃). Samples were washed three times in PBS and mounted as previously described. For invasion assays, Matrigel at a stock protein concentration of about 8 mg/ml was used directly or diluted to 1 mg/ml and supplemented with 1–20 μg/ml purified Col VI. In other cases, Col I gels were produced at a concentration of 1 mg/ml and similarly supplemented with 1–20 μg/ml Col VI.

Immunocytochemistry and FACS

Cells to be stained were washed twice in PBS with 0.1% BSA and fixed with 4% PFA for 10 min. Fixed cells were further washed in PBS and sequentially incubated with 2% (*v*/*v*) non-immune goat serum (Life Technologies Inc.) in PBS-BSA, primary and secondary anti-mouse or anti-rabbit antibodies (Alexa Fluor-conjugated; Life Technologies Inc.) diluted 1:100 in PBS-BSA, for 1 h each at room temperature. Cell nuclei were (counter)stained with either TO-PRO-3 (Life Technologies, Inc) or DAPI and immunostained specimens were mounted with Mowiol 4-88 (BD

Biosciences) supplemented with 2.5 mg/ml DABCO (Sigma-Aldrich) anti-fading reagent. FACS analyses were carried out primarily with the anti-NG2 PE-conjugated antibody 7.1 (Beckman-Coulter) and the corresponding isotype matched control antibody. Immunosorting of $NG2^+$ and $NG2^-$ sarcoma cells was accomplished by MACS-based magnetic bead separation using either the anti-NG2 antibody 9.2.27 (Millipore Corp.), or one of our recently generated anti-NG2 monoclonal antibodies mAb 2161D3, followed by incubation with goat anti-mouse IgG microbeads (Milteny Biotech, Inc). Relative efficiency of the immunosorting procedure and approximate yield of $NG2^+$ cells was on average 23.4% for MG63 cells, 13.6% for HT1080 cells, and 18.7% for SKUT-1 cells.

Transfection constructs and gene transduction

Human NG2 cDNA clones B, C and D (Pluschke et al., 1996) were cut with *Xho*I and *Sac*I, *Sac*I and *Hin*dIII, *Hind*III and *Bam*HI, respectively. These fragments were ligated and inserted into the pEGFP-N1 vector (Clontech Laboratories Inc.), and the sequence of the entire insert comprising bases 4030-7216 of the CSPG4 sequence reported with the NCBI accession number X96753 was verified by automated DNA sequencing. Dominant-negative-like mutant cells named $NG2^{cyto}$ were generated by treatment of cells stably transduced with a deletion construct encompassing the transmembrane domain and cytoplasmic tail of NG2 with the 3'-end-directed siRNA probe NG21279 to specifically abrogate the constitutively produced NG2 and spare the transduced deletion construct. Dominant-negative mutant cells (with respect to the putative signal transducing activity of NG2 upon extracellular ligand binding) named $NG2^{extra}$ were analogously generated by stable transfection of the same cell lines with a GFP-plasmid containing the entire extracellular portion and the transmembrane domain of human NG2. For this purpose, NG2 cDNA clones H, G and F 29 were cut with *Xho*I and *Apa*I, *Apa*I and *Bam*HI, *Bam*HI and *Hin*dIII, respectively, and inserted between the *Xho*I and *Hin*dIII sites into the pEGFP-N1 vector (BD Biosciences Inc.). Total cDNA from A375 melanoma cells was used as the template to amplify the sequence corresponding to nucleotides 2230-5025. The fragment was inserted into a pGEM-T vector (Promega), and its sequence was verified by automated DNA sequencing. The construct was then subcloned into the pEGFP-N1 expression vector containing fragments H, G and F as described above (BD Biosciences Inc.). Cells stably transfected with this plasmid were treated with a 5'-end-directed NG2 siRNA probe ($NG2^{C\text{-}terminus}$) to differentially eliminate the endogenous NG2 without affecting the transduced deletion construct. In both types of dominant-negative mutants, relative levels of expression of the full-length endogenous NG2 following siRNA knock-down, versus transduced truncated NG2 were determined at the mRNA level by quantitative real-time PCR as described above, FACS, and immunoblotting (Cattaruzza et al., 2012). Deletion constructs lacking different

segments of the putative extracellular region of the PG involved in Col VI binding were as previously described (Tillet et al., 1997; Burg et al., 1997).

Cell adhesion and migration assays

Adhesion of siRNA-treated and untreated cells to various purified ECM components was examined using a previously detailed cell adhesion assay denoted CAFCA (Centrifugal Assay for Fluorescence-based Cell Adhesion; Spessotto et al., 2009), which allows for both qualitative and quantitative parameters of cell-substratum adhesion to be established. Briefly, 6-well strips of flexible polyvinyl chloride–denoted centrifugal assay for fluorescence-based cell adhesion (CAFCA) miniplates covered with double-sided tape (bottom units) were coated with 20 μg/ml of interested protein.

Cells were labeled with the vital fluorochrome calcein acetoxymethyl (Invitrogen) for 15 min at 37 ℃ and were then aliquoted into the bottom CAFCA miniplates, which were centrifuged to synchronize the contact of the cells with the substrate. The miniplates were then incubated for 20 min at 37 ℃ and were subsequently mounted together with a similar CAFCA miniplate to create communicating chambers for subsequent reverse centrifugation. The relative number of cells bound to the substrate (i.e., remaining in the wells of the bottom miniplates) and cells that failed to bind to the substrate (i.e., remaining in the wells of the top miniplates) was estimated by top/bottom fluorescence detection in a computer-interfaced GENios Plus microplate reader (Tecan Group Ltd.). In assays involving signalling antagonists, immunosorted $NG2^+$ and $NG2^-$ cells and siRNA-treated cells were confronted with Col I and Col VI substrates in the presence of the following inhibitors: calphostin-C (PKCα; at 50 nM), UO126 (MEK1/MEK; up to 10 μM), UO124 (control drug for MEK1/MEK2 inhibitors; up to 10 μM), SB203580 and PD169316 (p38MAPK; up to 10 μM), suramin (CAMK; at 1 μM), PP2 (Src; up to 1 nM), okadaic acid (PP1 and PP2A; up to 10 μM), SB216763 (GSK3α; up to 10 μM), SB202474 (control drug for MAPK inhibitors; up to 10 μM), Y27632 (ROCK-1; up to 10 μM), LY294002 (PI-3K; up to 10 μM), Wortmannin (PI-3K; up to 5 μM), GDC-0941 (p110α; up to 1 μM), TGX-221 (p110β; up to 1 μM) and AS252424 (p110γ; up to 5 μM), obtained from Sigma-Aldrich, Merck Laboratories-Calbiochem Research, Santa Cruz Biotechnology Inc, Enzo Life Sciences AG, and Axon Medchem. Drug doses were initially calibrated through cytotoxity tests on the specific sarcoma cells. Optimal doses were next established through proliferation assays with pre-starved cells plated on Col VI or fibronectin. We then performed pilot migration tests that revealed many of the agents indiscriminately affecting the process of locomotion on both the NG2-dependent Col VI substrate and NG2-independent substrates such as Col I and fibronectin. We therefore applied our CAFCA system to evaluate the

role of the phoshorylations induced by the NG2-Col VI interaction in the context of short-term cell-substrate adhesion. This was done using immunosorted $NG2^+$ and $NG2^-$ cell subsets and siRNA-treatred cells. Scratch-based migration assays were then also performed in the presence of PI-3K inhibitors. For evaluation of cell attachment dynamics to native matrices deposited *in vitro* by embryonic fibroblasts isolated from wild and Col VI null mice, sarcoma cells within representative areas of the matrix substrate were inspected at 15 and 30 min after plating for their morphology, prior to (by phase-contrast microscopy) and after staining for actin microfilaments and vinculin. In these experiments the number of cells plated was of 1×10^5/well in 24-well plate. At the indicated time points, the matrix was rinsed two times with DPBS to wash out the unattached cells and then we fixed all with 4% PFA for 20 min at room temperature and washed two times with DPBS. Assessments of cell binding to native matrices were carried out in triplicate from three independent experiments by cell counting under phase contrast microscopy adopting 15–20 different representative fields of the substrate with visible matrix deposits. Parallel substrates of purified Col VI were used as reference. Cell migration and invasion assays were carried out using a modified version of FATIMA (fluorescence-assisted transmigration, invasion and motility assay; Spessotto et al., 2009). For this purpose, FluoBlock inserts (BD Biosciences) with fluorescence shielding membranes carrying 8 μm pores were coated with either purified ECM components, Matrigel or polymerized on their lower or upper side. In the case of Matrigel and Col I solutions, these were diluted in cold serum-free DMEM medium at a concentration of 0.5–1 mg/ml and 50 μl of the solution was dispensed onto the porous membrane. FluoBlock inserts were then incubated for 1 h at 37℃ to form a semisolid thin gel across the membrane. siRNA-treated and untreated cells were fluorescently tagged with FAST Dil (Life Technologies Inc) as previously described (Spessotto et al., 2009) and plated at a density of 5×10^5 cells in 500 μl of DMEM containing 0.1% BSA onto the coated membranes and grown on this substrate for up to 24 h. The lower compartment of the inserts was filled with 1.5 ml of DMEM with 0.1% BSA. The percentage of transmigrated and "stationary" cells was assessed using the SPECTRA Fluor microplate fluorometer (TECAN Group). Haptotactic migration of siRNA-treated and untreated cells in response to purified EMC molecules was examined by coating overnight at 4℃ the lower side of the porous membranes with 20 μg/ml of rat tail Col I and Col VI, both diluted in 0.05 M bicarbonate buffer, pH 9.6. For video-time lapsed scratch-assay, seeded cells were allowed to reach confluence, the monolayer was starved over-night in 1% FCS, or for 48 h in experiments involving the use of signalling blockers, and wounded with a pipet tip. After scraping the cells were rinsed twice with PBS to removed cell-aggregates and debris. After soluble addition of Col VI (20 μg/ml) in DMEM with 0.5% of serum, real-time video microscopy was done with an inverted phase-contrast microscope (Leica) equipped with an on-

stage mini-chamber providing routine incubation conditions (37℃, 5% CO_2). Phase-contrast images were taken at 5 min intervals, contrasted digitally and exported into conventional image analyses software for elaboration and presentation. For video display image stacks were compressed and processed as Quick Time movies. Quantification of migratory parameters such as speed of movement, vectorial directional persistency and distance migrated by individual cells were accomplished using the dedicated software provided with the microscopic Leica system.

Phospho-proteomic profiling and functional follow-up screening

Through the antibody array approach, platforms of 1278 antibody spots were adopted to comparatively examine 627 signal transduction components in duplicate. The platform comprises 273 antibodies directed against specific phosphorylation sites and 378 antibodies recognizing the cognate antigens in any phosphorylation state. Since cell binding to Col VI substrates was strongly compromised in cells with abrogated NG2, it was not technically possible to use an experimental paradigm involving direct plating of the cells onto Col VI substrates. A similar technical caveat was encountered in the context of cell binding to Col I after ablation of β1-integrins (i.e. substrate adhesion was strongly impaired; not shown). Furthermore, because of the confounding intracellular signals that could be elicited by unrelated substrate molecules introduced into the system, it was not possible to use cells bound to a different "NG2-independent" substrate rather than Col VI (or to a mixture of Col VI and another ECM component), and then add Col VI to the system. This forced us to use an alternative paradigm for efficiently accomplishing our four-way comparative analysis. Thus, in the first series of experiments SK-UT-1 $NG2^+$ and $NG2^-$ cell subsets were treated with a β1 integrin-directed siRNA probe (Tebu-bio Lab), which was independently validated for efficiency by flow cytometry (Supplementary Figure S6) and cell adhesion on fibronectin. Cells were starved for 24 h in culture medium containing 0.5% FCS, plated on poly-L-lysine (0.1% coating), treated with a function-blocking antibody against the α2 integrin subunit (kindly provided by Luigi De Marco, The National Cancer Institute Aviano), and incubated for 30 min with molar equivalents of Col I (160 μg/ml) or tetrameric Col VI (20 μg/ml). Cells were lysed in the presence of protease inhibitors and the lysates were processed by semi-quantitative immunoblotting with the KPSS 1.3 phosphosite screen. For this purpose an amount of 600 μg whole cell lysate per sample from collagen-exposed $NG2^+$ and $NG2^-$ cells was prepared according to the instructions provided by the service company. Briefly, after removal of the medium, cells were rinsed in dish with ice-cold PBS once, detached with trypsin, and followed by the addition of equal volume of medium. Cells were collected in a 15-ml conical tube and centrifuged at 500× *g* for 2 min at 4℃. The pellets were washed twice with ice-cold PBS and ice-cold lysis buffer was then added. After cell scraping, the liquid was collected,

sonicated four times and assayed for protein concentration. Samples (2 mg/ml) were then frozen. In the subsequent series of experiments, we used B16 murine melanoma cells stably transfected with rodent NG2 and compared these cells with mock-transfected ones using the same collagen-induction paradigm (Supplementary Figure S6) and Western blotting-based phosphosite screening described above. Prior to the exposure to Col I and Col VI, cells were incubated with anti-murine β1 integrin-directed siRNA probe (Santa Cruz Biotechnology), which was similarly validated in our system by flow cytometry and cell adhesion to fibronectin. For global phosphosite/proteomic analyses we used the experimental set up described above involving SK-UT-1 $NG2^+$ and $NG2^-$ cells and the antibody microarray platform. The 18 phosphorylation sites found to be most divergent according to the hierarchical clustering were next confirmed by semi-quantitative immunoblotting (Kinetworks™ Hit Validation Service, Kinexus Bioinformatic Corp.) and in a number of cases by western blotting performed in-house using the antibodies indicated by the company. For western blot analysis of PI-3K phosphorylation, whole cell lysates were resolved by SDS-PAGE on 4%–12% gradient gels (Bio-Rad Laboratories, Inc) under reducing conditions and transferred to nitrocellulose membranes. The membranes were saturated with 5% BSA in TBST for 1 h at room temperature and incubated with primary antibodies 9.2.27 (anti-NG2), anti-β-actin antiserum (ABCAM), and anti-PI-3K p110α or PI-3Kp85 (Tyr458) polyclonal antisera (Cell Signaling Technology, Inc.) at 4℃ overnight. Membranes were then washed and incubated with peroxidase-labeled goat anti-rabbit or anti-mouse antibodies (Life Technologies) followed by chemiluminescent detection using the ECL Plus kit (Amersham Biosciences).

In vivo tumorigenesis

In pilot tests we performed a dose-escalation analysis of the number of implanted cells needed to obtain detectable subcutaneous tumour lesions and assayed implantations ranging from 1×10^6 to 5×10^6 cells/flank/animal co-injected with Matrigel at a protein concentration of >5 mg/ml. Mice receiving unilateral subcutaneous tumour cell implantations were 7 weeks of age at the time of the implant and were monitored by visual inspection at 2 days intervals for up to 65 consecutive days. For end-point evaluations of tumour formation, we adopted an arbitrary scoring based upon assessment of three primary parameters, i.e. transplanted cell dose, final size of the tumour lesion and latency of tumour formation (i.e. number of days needed to generate a tumour mass of the allowed size; see below). Scoring values were defined accordingly using the formula: fraction number of inoculated cells (expressed as number of millions of cells, ranging from 1 to 1/5) × final tumour volume (cm^3) at time of euthanizing divided by number of days of tumour growth: score 0 = no engraftment/growth (values = 0–0.00045); score 1 = minimal tumour mass (values = 0.00046–

0.00409); score 2 = small tumour mass (values = 0.00410–0.00773); score 3 = medium-sized tumour mass (values = 0.00774–0.01138); and score 4 = large tumour mass (0.01139–0.01502). In another series of experiments a total of 93 nude mice (85 successfully evaluated) were subcutaneously inoculated with 1×10^6, 3×10^6 or 5×10^6 immunosorted $NG2^+$ or $NG2^-$ STS cells (unsorted cells were used as reference for each experiment) suspended in Matrigel and implanted unilaterally into the flank of the animals as described above. In some cases, comparable bilateral subcutaneous implantations were done using $NG2^+$ and $NG2^-$ cells for each of the flanks. In comparative analyses of tumour formation/growth of $NG2^+$ versus $NG2^-$ cells, all animals were euthanized at the time that any of subjects manifested signs of morbidity or tumour masses had reached over sizes of 1.5–2.0 cm in diameter. Euthanized animals were subjected to macroscopical evaluation and photographic documentation of the tumour lesions, and eventually processed by autopsy to verify tumour cell infiltrations in primary organs. During the period of the experiments, animals were taken further care to ensure that the tumour burden did not obviously impair the primary needs, i.e., ambulation, eating, drinking, defecating, and urinating. Tumour masses that formed in manipulated animals were regularly excised and in most cases subjected to histological and immunohistochemical analyses.

References

Hedman, K., Kurkinen, M., Alitalo, K., et al. (1979). Isolation of the pericellular matrix of human fibroblast cultures. JCB. *81*, 83-91.

Moore, H.M., Kelly, A.B., Jewell, S.D., et al. (2011). Biospecimen reporting for improved study quality (BRISQ). J Proteome Res. *10*, 3429-3438.

Pluschke, G., Vanek, M., Evans, A., et al. (1996). Molecular cloning of a human melanoma-associated chondroitin sulfate proteoglycan. Proc. Natl. Acad. Sci. USA. *93*, 9710-9715.

Spessotto, P., Lacrima, K., Nicolosi, P.A., et al. (2009). Fluorescence-based assays for in vitro analysis of cell adhesion and migration. Methods Mol Biol. *522*, 221-250.

SUPPLEMENTARY TABLE

Supplementary Table S1. *Demographics and baseline clinical traits of STS patients from whom surgical specimens were subjected to molecular analyses*[1]

Patient	Sex	Age	Histological subtype[2]/grade[3]	Site of primary lesion	Site of metastases	Clinical course[4]
1	M	72	MFS/II	Thigh	Lymphnodes	DOD
2	M	54	MFS/II	Leg	NF	NED
3	M	63	MFS/III	Thigh	NF	NED
4	M	61	MFS/II	Shoulder	Lung	AWD
5	F	73	MFS/III	Thigh	Lung	AWD
6	F	54	MFS/III	Thigh	Lymphnodes	DOD
7	M	64	UPMS/III	Thigh	Lung	DOD
8	M	62	UPMS/III	Arm	NF	NED
9	M	38	MFS/III	Thigh	NF	NED
10	F	43	UPMS/III	Thigh	NF	NED
11	F	67	UPMS/III	Pelvic girdle	NF	DOD
12	F	72	UPMS/III	Thigh	Lung	DOD
13	F	56	UPMS/III	Thigh	Lung	DOD
14	M	38	UPMS/III	Thigh	Lung	DOD
15	M	62	UPMS/III	Pelvic girdle	Lung	NED2
16	F	66	UPMS/III	Thigh	Lung	DOD
17	M	71	LMS-c/III	Thigh	Lung	DOD
18	M	57	LMS-c/III	Forearm	Lung	AWD
19	M	63	LMS-p/III	Arm	Lung	DOD
20	F	76	LMS-p/III	Thigh	Lung	DOD
21	M	34	LMS-p/III	Thigh	Lung	DOD

22	M	62	LMS-c/III	Thigh	Lung	DOD
23	M	66	LMS-c/III	Forearm	Lung	AWD
24	M	34	LMS-p/III	Spine	Lung	DOD
25	M	55	LMS-c/III	Thigh	Lung	DOD
26	M	68	LMS-c/II	Leg	Absent	NED
27	M	38	LMS-p/II	Leg	NF	NED
28	F	61	LMS-p/III	Thigh	Lymphnodes	AWD
29	M	43	LMS-p/III	Thigh	Lung	AWD
30	M	52	LMS-p/III	Thigh	Lung	DOD
31	F	79	LMS-c/II	Thigh	NF	DOD
32	F	57	LMS-c/III	Thigh	Lung	DOD
33	M	76	LMS-p/III	Thigh	Lung	DOD
34	F	66	LMS-p/III	Leg	NF	DOD
35	F	68	LMS-p/III	Thigh	Lung	DOD
36	F	54	LMS-c/III	Thigh	Viscera	DOD
37	F	42	LMS-c/III	Thigh	Lung	DOD
38	F	71	LMS-p/III	Leg	Lung	NED2
39	F	38	LMS-c	Leg	Lung	AWD
40	F	41	LMS-c	Thigh	Bone	DOD
41	F	40	LMS-c	Thigh	NF	NED
42	M	65	LMS-p	Leg	Lymphnodes	AWD
43	M	73	LMS-p	Thigh	Lymphnodes	NED2
44	M	72	LMS-p	Thigh	NF	NED
45	M	50	LS-p/II	Thigh	Lung	AWD
46	M	42	LS-p/II	Thigh	NF	AWD
47	M	56	LS-p/III	Leg	Liver	AWD
48	M	59	LS-p/III	Thigh	Bone	DOD

49	M	47	LS-p/II	Leg	NF	NED
50	F	73	LS-p/II	Thigh	NF	NED
51	F	49	LS-p/II	Thigh	NF	NED
52	F	40	LS-p/II	Leg	NF	NED
53	M	72	LS-p/III	Thigh	NF	DOD
54	F	54	LS-dd/II	Thigh	NF	NED
55	M	63	LS-dd/III	Thigh	NF	DOD
56	F	61	FS/III	Forearm	Lung	DOD
57	M	73	FS/III	Trunk	NF	NED
58	F	54	FS/III	arm	Lung	DOD
59	M	64	FS/III	Trunk	Lung	DOD
60	M	62	FS/IIB	Forearm	NF	NED
61	F	38	FS/III	Knee	NF	NED
62	M	43	LS-rc/III	Thigh	Bone	DOD
63	M	67	LS-rc/III	Thigh	Lung	DOD
64	F	72	LS-rc/II	Leg	NF	NED
65	M	46	LS-rc/III	Thigh	Lung	NED2
66	M	38	LS-rc/III	Ischium	Lung	NED2
67	F	62	LS-rc/III	Thigh	Lung	DOD
68	M	66	LS-rc/III	Thigh	NF	NED
69	M	71	LS-rc/III	Leg	Lung	NED2
70	M	57	LS-rc/III	Thigh	NF	DOD
71	M	63	LS-rc/III	Thigh	NF	DOD
72	M	76	LS-rc/III	Leg	Lung	NED2
73	M	34	LS-rc/II	Thigh	NF	NED
74	M	62	LS-rc/III	Knee	Lymphnodes	DOD

75	F	66	LS-rc/III	Thigh	Lung	AWD
76	M	34	LS-rc/II	Thigh	NF	NED
77	M	55	LS-mx/II	Thigh	NF	NED
78	M	78	LS-mx/II	Leg	NF	NED
79	F	38	LS-mx/III	Thigh	Lymphnodes	NED2
80	M	61	LS-mx/II	Thigh	NF	NED
81	M	43	LS-mx/II	Knee	NF	NED
82	M	52	LS-mx/II	Leg	NF	NED
83	M	79	LS-mx/II	Thigh	NF	NED
84	F	57	LS-mx/III	Thigh	Lung	AWD
85	M	76	LS-mx/II	Thigh	NF	NED
86	M	66	LS-mx/II	Thigh	NF	NED
87	F	68	LS-mx/II	Thigh	NF	NED
88	M	74	LS-mx/II	Leg	NF	NED
89	M	42	LS-mx/II	Thigh	NF	NED
90	M	71	LS-mx/II	Thigh	NF	NED
91	M	38	LS.mx/II	Thigh	NF	NED
92	F	41	LS-mx/II	Thigh	NF	NED
93	M	40	LS-rc/III	Thigh	NF	DOD
94	M	65	LS-rc/III	Leg	Bone	DOD
95	F	73	LS-mx/II	Knee	Lung	NED2
96	F	72	LS-mx/II	Knee	Lung	NED2
97	M	50	LS-rc/III	Knee	Lung	DOD
98	M	42	SS	Knee	Lung	NED2
99	F	56	SS	Elbow	NF	NED
100	M	59	SS	Thigh	Lung	AWD
101	M	47	SS	Forearm	Lung	AWD

102	M	73	SS	Elbow	Bone	DOD
103	F	49	SS	Shoulder	Lymphnodes	DOD
104	F	40	SS	Forearm	Lung	NED2
105	M	42	SS	Thigh	NF	NED
106	M	55	SS	Thigh	Lung	NED2
107	F	63	SS	Forearm	NF	NED
108	M	75	SS	Thigh	Lung	NED2

[1]All specimens were collected under informed consent from STS patients who underwent surgical and post-surgical treatments at the Rizzoli Orthopaedic Institute;
[2]Histological subtypes and their variants were as follows: MFS, mixofibrosarcoma; UPMS, undifferentiated pleomorphic sarcoma of the storiform type; LMS-c, conventional leiomyosarcoma, of cutaneous or somatic soft-tissue type (depending upon the anatomical location); LMS-p, pleomorphic leiomyosarcoma; LS-pm, pleomorphic liposarcoma; LS-dd, dedifferentiated liposarcoma; LS-mx, myxoid liposarcoma; LS-rc, round-cell liposarcoma; FS, fibrosarcoma. SS monophasic synovial sarcoma.
[3]Tumor grading was according to that established by the American Joint Committee for Cancer and the French Fédération Nationale des Centres de Lutte contre le Cancer;
[4]As established at a 5 years follow-up: DOD, patients dead because of the disease; AWD, patients alive but with detectable disease; NED, patients with no evidence of disease; NED2, patients who relapsed but had a subsequent disease regression.
NF= no found

SUPPLEMENTARY FIGURES

Supplemental Figure 1

A

Variables	*Exp (B) (odds ratio)*	*95% CI*		*p*
		Inferior	*Superior*	
NG2 > 1000	1.41	1.03	1.94	0.03
Therapy	0.79	0.53	1.18	0.25
Site	0.95	0.65	1.37	0.77
Size>10	1.04	0.74	1.46	0.82
Age	0.98	0.96	1.03	0.09
Gender	1.27	0.88	1.81	0.18

B

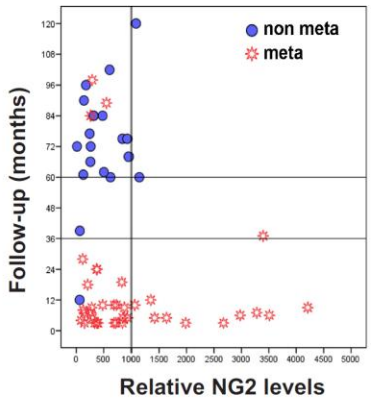

Supplementary Figure S1. (A) Summary of a Cox regression, multivariate analysis confirming the independence scoring of NG2 overexpression in metastatic lesions as a prognostic factor. "Therapy" refers to the type of post-surgery therapeutical intervention; "Size >10" refers to primary masses with a size larger than 10 mm. Patient cohort was homogenous with respect to grade, stage and mitotic index of the tumour lesions (see *Materials and Methods*). **(B)** Timing of detection of metastatic disease ("meta") in post-surgery STS patients as a function of the NG2 transcriptional levels in their primary lesions ("non meta" refers to metastasis-free patients).

Supplemental Figure 2. NG2 and Col VI expression pattern of STS cells.

Designation	Patient code	Histological subtype	NG2 expression levels (%)[a]	Col VI expression[b]
SK-LMS-1	NA	Leiomyosarcoma	88.5	+
SK-UT-1	NA	Leiomyosarcoma	63.6	+
MES-SA	NA	Leiomyosarcoma	58.3	–
MG63	NA	Osteosarcoma	83.5	–
SW982	NA	Synovial sarcoma	26.3	–
GCT	NA	Fibrous histiocytoma	47.8	+
HT1080	NA	Fibrosarcoma	37.5	+
143B	NA	Osteosarcoma	61.8	–
SW872	NA	Liposarcoma	99.4	+
RD/KD	NA	Rhabdomyosarcoma	43.2	–
A375	NA	Melanoma	91.2	n.d.
NT-LS-1[c]	91818	Liposarcoma	34.1	–
NT-LS-2	108876	Liposarcoma	0.9	–
NT-LS-3	110543	Liposarcoma	1.7	–
NTI-MFH-1	97441	Fibrous histiocytoma	1.0	–
NTI-MFH-3	98337	Fibrous histocytoma	51.6	–
NTI-OS-2	128246	Osteosarcoma	81.2	–
NTI-LMS-1	94278	Leiomyosarcoma	76.8	–
NTI-LMS-2	95058	Leiomyosarcoma	37.5	–
NTI-LMS-4	98035	Leiomyosarcoma	2.3	–
NTI-LMS-7	109541	Leiomyosarcoma	11.8	+
NTI-FS-1	91266	Fibrosarcoma	32.4	+++

[a]determined by FACS analysis; [b]determined by combined PCR and immunocytochemistry; [c]cells isolated in the laboratory from specimens derived from STS patients that underwent surgical removal of primary and secondary (lung metastases) lesions at the National Tumour Institute of Aviano

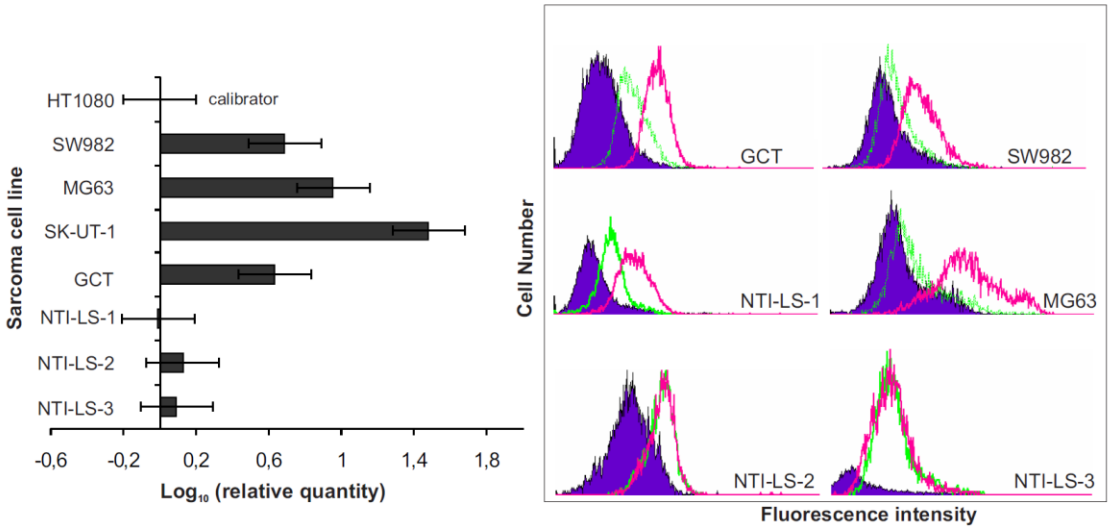

Supplementary Figure S2. *Upper table* summarizes the histological subtype derivation and the corresponding NG2 surface levels and Col VI secretion patterns in a panel of established sarcoma cell lines and primary sarcoma cells isolated in the laboratory from relapsing and metastatic lesions.

Percentages of NG2 expression refer to the relative amount of cells within the analyzed population expressing detectable levels of NG2 in one flow cytometry analysis performed in triplicate. A375 melanoma cells were used as reference because of their reportedly high levels of NG2 expression. Col VI secretion abilities were established by combined assessment of the relative levels of the α3(VI) chain mRNA and by semi-quantitative evaluation of the immunostaining patterns obtained with a propriety anti-Col VI antiserum. *Lower graphs* show assessment of gene transcription (*left*) and protein translation (*right*) of NG2 in a selected number of sarcoma cell types, as determined by qPCR and flow cytometry.

Supplemental Figure 3

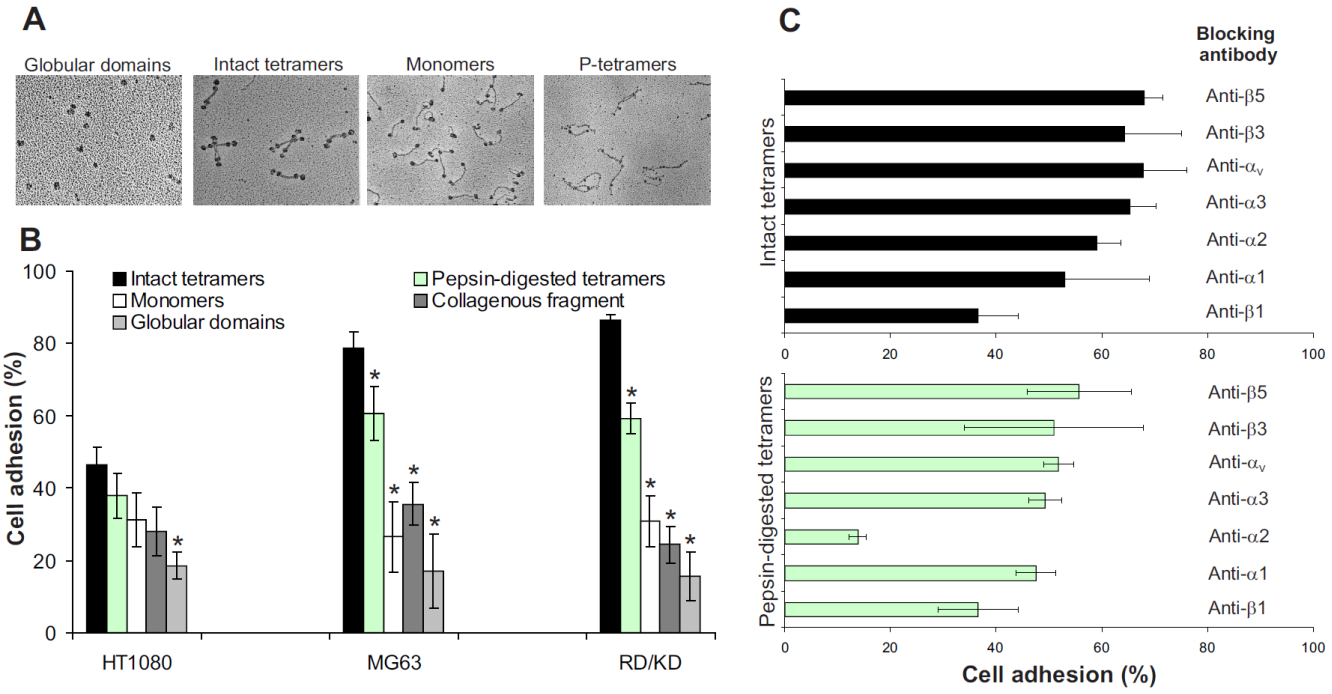

Supplementary Figure S3. (A) Adhesion patterns of three of the sarcoma cell lines used in this study when assayed on various forms of Col VI. These included intact tetrameric units of the collagen (*Intact tetramers*), monomeric forms of the collagen (*Monomers*), pepsin-digested tetramers (*P-tetramers*; i.e. tetrameric forms of the collagen lacking the *N*- and *C*-terminal globular domains of each of the constituent chains), a tetrameric fragment embodying only the collagenous portion of the molecule (*Collagenous fragment*) and the separated *N*- and *C*-terminal globular domains (*Globular domains*). Upper photographs (*inset*) show representative TEM/rotary shadowing images of these different forms of the collagen that were assayed. **(B)** Integrin involvement in the attachment of the rhabdomyosarcoma cell line RD/KD to intact tetramers of Col VI (*upper graph*), or pepsin-digested tetramers (*lower graph*), as determined by the use of function-blocking antibodies against discrete integrin subunits. The RD/KD cell line was chosen as reference for these assays because of its high expression of α2β1 integrin. Similar results were obtained with HT1080 and MG63 cells.

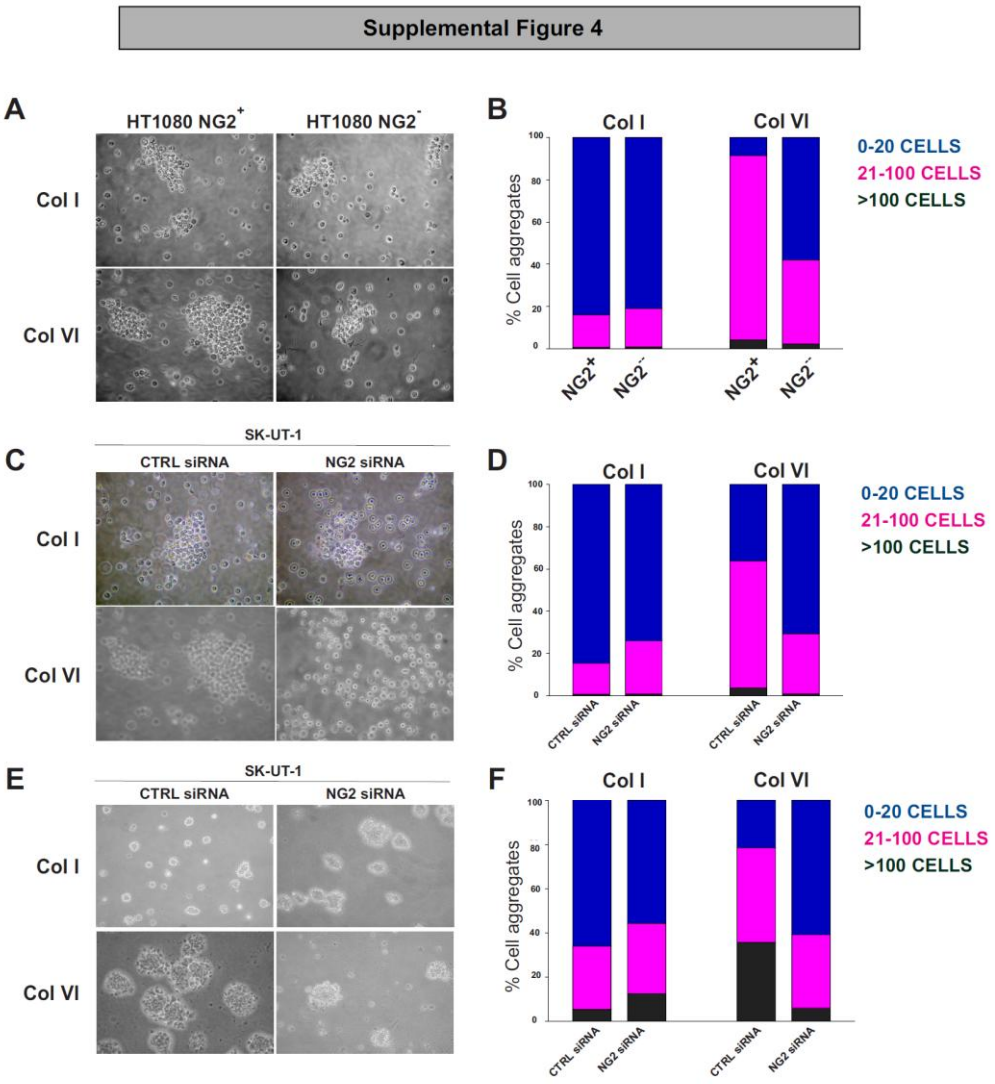

Supplementary Figure S4. Representative phase-contrast images **(A, C)** and assessment of cell-cell aggregation **(B, D)** induced by either Col I or Col VI (both added in solution) in immunosorted HT1080 $NG2^+$ and $NG2^-$ cells, or SK-UT-1 cells treated or not with anti-NG2 siRNAs (x20 magnification). Graphs report the relative frequency of cellular aggregates composed of the indicated amount of cells, when averaged from three independent experiments with an overall SD of <20%. **(E)** Representative phase-contrast images (*left panels*) of anchorage-independent colony formation in soft-agar in the presence of either Col I or Col VI and the corresponding assessment **(F)** of the percentages of colonies with different amounts of cells (averaged from quadruplicate experiments with SD ± 25%). In all cases, higher order cellular aggregates (colonies, i.e. aggregates composed of >20 cells), were significantly different in $NG2^+$ versus $NG2^-$ cells in the presence of Col VI and when comparing the behaviour of cells in the presence of Col I (p<0.0005-0.001 by Mann-Whittney U test).

Supplemental Figure 5

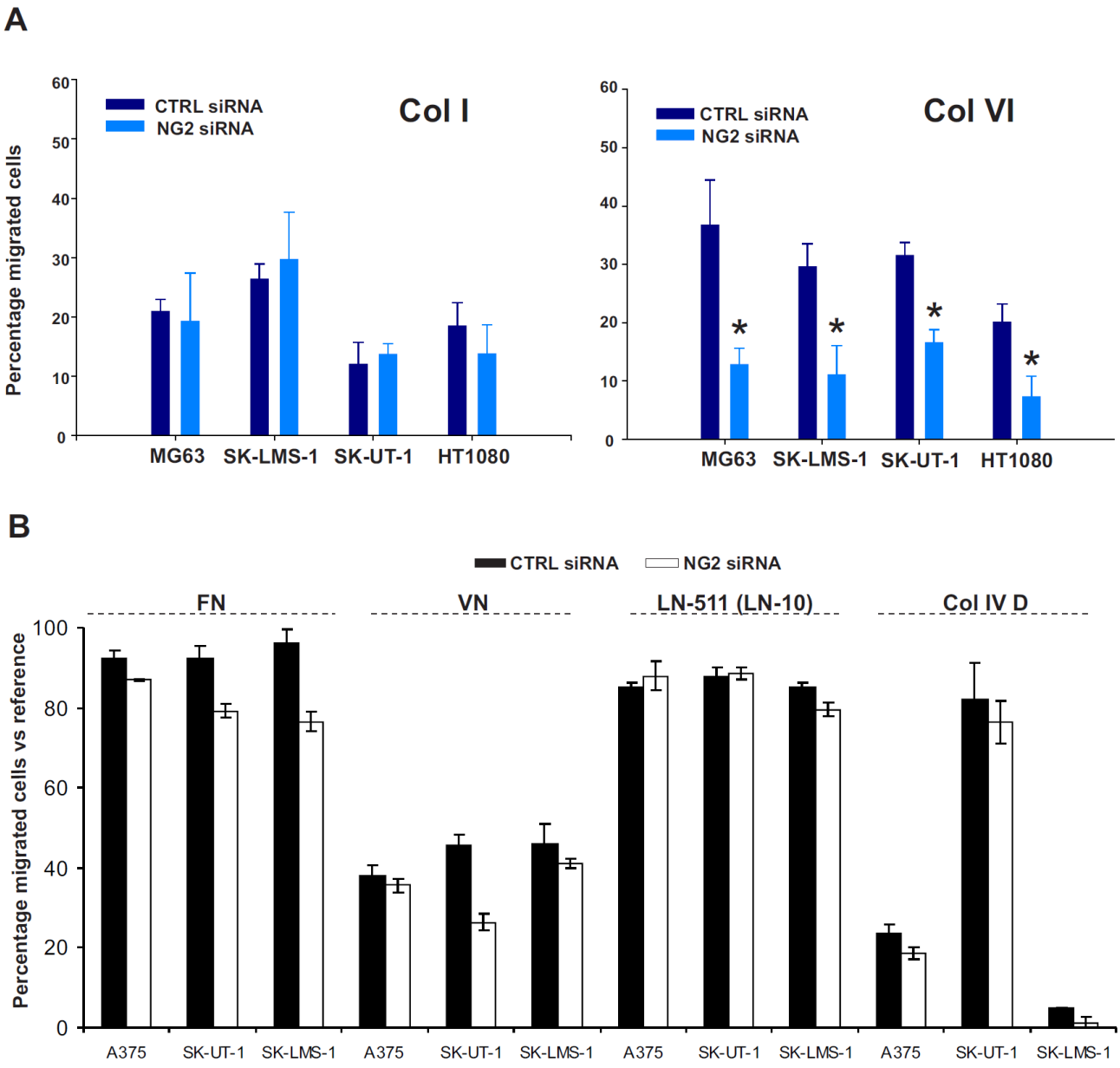

Supplementary Figure S5. (A) Extent of haptotactic cell migration in response to Col I or Col VI of different sarcoma cell lines in which NG2 was knocked down ("*", $p<0.0054$ by two-way ANOVA). **(B)** Lack of NG2-dependence in sarcoma cell adhesion to different representative ECM substrates, including fibronectin (FN), vitronectin (VN), laminin isoform 511 (LN-511) and collagen type IV (Col IV D, dimeric variant).

Supplemental Figure 6

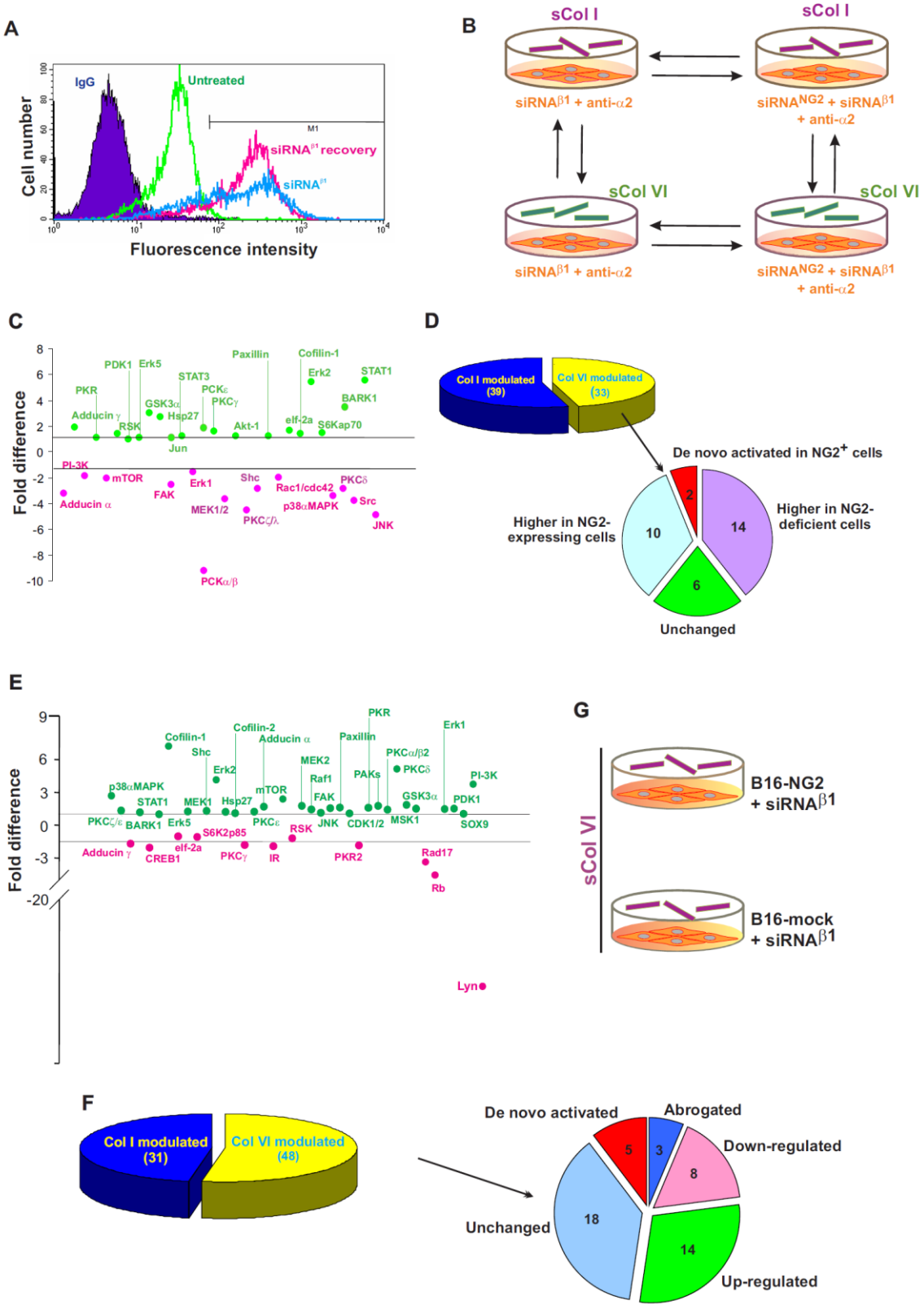

Supplementary Figure S6. (A) Relative levels of transient β1 integrin subunit knockdown (as determined by flow cytometry) in SK-UT-1 cells and time-dependent surface recovery (siRNA$^{\beta1}$ recovery) of the integrin. Knockdown efficacy of the siRNA probe was evaluated 3 days following transfection and surface recovery after additional 3 days (i.e. a total 6 days after transfection). A sequence scrambled siRNA probe was used as a negative control. Anti-human and anti-murine β1 integrin siRNA probes were also independently validated for their ability to inhibit cell binding to FN by at least 50% (*not shown*). **(B)** Strategy employed for the four-way comparative phospho-proteomic profiling (as depicted by the arrows) based upon semi-quantitative Western blotting with a total of 69 antibodies against phosphorylation sites within 64 signal transduction components. Starved cells were exposed for 30 min to molar equivalents of monomeric Col I and intact Col VI tetramers (i.e. 160 μg/ml of Col I monomers and 20 μg/ml of Col VI tetramers), following knockdown of the β1 integrin subunit and NG2 ("NG2-deficient"). Cells were then lysed and the solubilised material resolved by SDS-PAGE under reducing conditions and processed for immunoblotting. **(C)** The plot summarizes the variations in phosphorylation degree of the indicated molecules when comparing cells treated with the NG2-directed siRNA versus control siRNA probe and after normalization against the variations observed when comparing Col I- versus Col VI-exposed cells. No significant differences in phosphorylation levels were observed in cells exposed to Col I. Differences in phosphorylation degree were determined by adopting an arbitrary ±1.5 fold-difference to define significantly up- or down-regulated phosphorylation levels after normalization to the relative amount of the molecules detectable in either cell phenotype/condition. The accompanying pie chart **(D)** summarizes the total outcome of the phospho-proteomic screening using the same comparative criteria and threshold as in **(C)**. Summary plot **(E)** and global pie chart **(F)** of the final outcome of an alternative phospho-proteomic screening carried out according to the scheme depicted in **(G)** and entailing murine B16 melanoma cells stably transduced to express rodent NG2 ectopically. NG2-transfected and mock-transfected cells were treated with a mouse-specific siRNA to knockdown the β1 integrin subunit and exposed for 30 min to soluble Col VI tetramers. Lysates of the cells were processed for phospho-proteomic analysis as described above.

Supplemental Figure 7

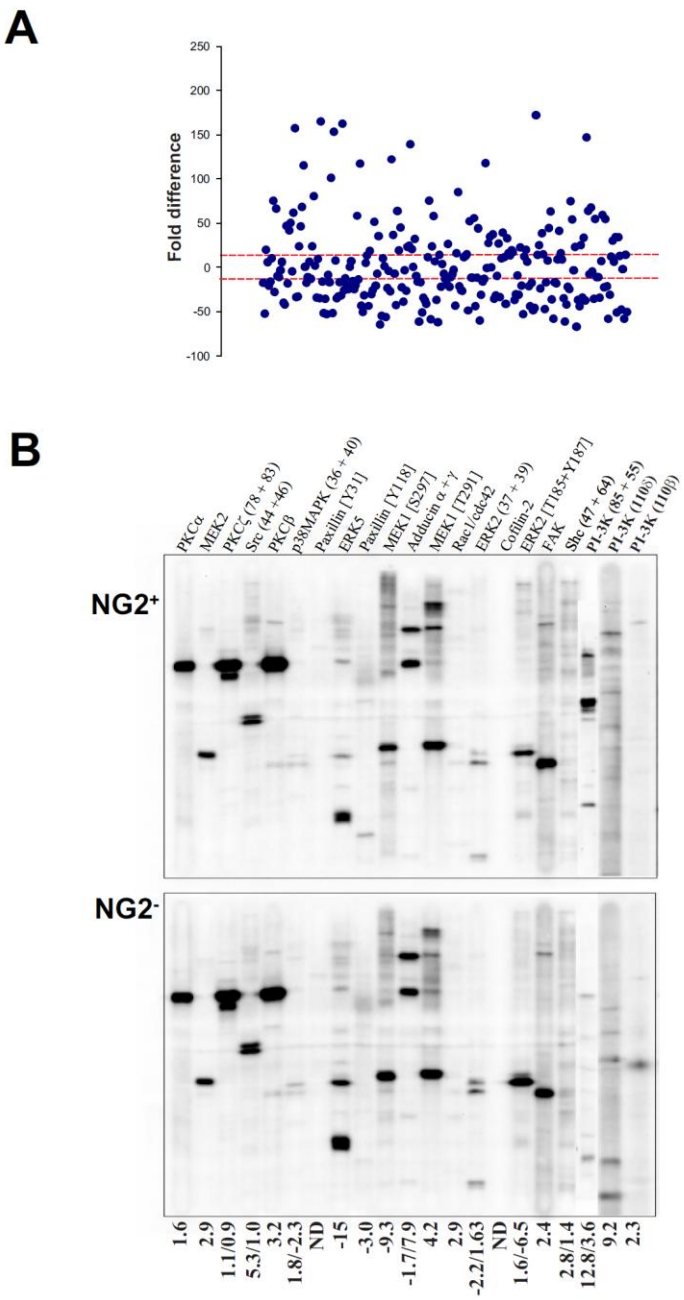

Supplementary Figure S7. (A) Comprehensive outcome of the phospho-site screening performed through fluorescent antibody arrays in NG2-positive versus NG2-negative HT1080 cell subsets confronted with Col VI. The plot reports the relative fold difference in the levels of phosphorylation of

the components/phosphosites detected in the two cell phenotypes (*positive values* refer to higher phosphorylation levels in NG2-positive cells when compared to NG2-negative ones, whereas the opposite relationship is for *negative values*). **(B)** Confirmatory semi-quantitative immunoblotting of a prioritized selection of the 21 most modulated signalling components identified through the antibody array screening. Phosphosites indicated within squared brackets are the ones specifically detected for the given molecule. Numbers reported within normal brackets refer to different isoforms of the detected molecule. Numbers reported below the blots indicate the fold differences in phosphorylation degrees between NG2-positive and NG2-negative cells as determined by densitometric analysis. The first and second value refer to the larger and smaller isoform indicated within the brackets for the given molecule (*see above*). Positive values refer to fold differences in band intensity when comparing $NG2^+$ versus $NG2^-$ cells, whereas negative values refer to the opposite situation. Protein loading normalization was carried out using F-actin and normalization of the phosphorylation pattern was performed using β-tubulin as a calibrator.